Effect of temperatures variation on the synthesis and characterization of cerium oxide nanoparticles by co-precipitation method

Y. Arooj [a], R. Karim [b], S. Maqsood [a,c], A. Farhan [b], A. Kahlid [b], A. Erum [a], M. A. Qamar [d,1*]

[a] *Department of Physics, Government College Women University Faisalabad, Faisalabad 38000, Pakistan*

[b] *Department of Chemistry, University of Agriculture Faisalabad, Faisalabad, Pakistan*

[c] *Department of Physics, University of Agriculture Faisalabad, Faisalabad, Pakistan*

[d] *Department of Chemistry, School of Science, University of Management and Technology, Lahore 54770, Pakistan*

In the current study, cerium oxide (CeO_2) nanoparticles (NPs) were synthesized and investigated because of their outstanding optical, electrical, structural, and morphological properties. CeO_2 NPs were formed by a simple, low-cost, and eco-friendly co-precipitation method. The effect of calcination temperature on nanoceria was examined through X-ray diffraction (XRD), scanning electron microscope (SEM), Fourier Transform Infrared spectroscopy (FTIR), Ultraviolet and Visible spectroscopy (UV–Vis), and the current voltage (I-V) studies. The XRD revealed the FCC structure and crystallite size in the 60-90 nm range when the calcination temperature was increased. SEM showed spherical particles with significant agglomeration. FTIR showed the occurrence of the Ce-O bond. UV-Vis showed the value of 236 nm maximum absorption wavelength with a 3.27 eV band gap. PL showed a 651 nm emission band with a 1.90 eV energy band gap. Raman examined the cubic structure of nanoceria. The current voltage (I-V) studies examined the dependence of resistivity on calcination temperature.

(Received February 11, 2025; Accepted May 25, 2025)

Keywords: Cerium oxide, FCC structure, Co-precipitation, Raman spectra

1. Introduction

Materials that have a single dimension within a 1-100 nanometer range are referred to as nanomaterials [1]. Science society has a great interest in these nanomaterials because of their wide range of applications. This is often called “the next industrial revolution” [2]. Nanoparticles are fundamental components of nanotechnology and exhibit distinct optical, magnetic, and electrical characteristics [3]. All these properties are different from bulk particles. Because of this, nanoparticles receive a lot of interest in research area. Semiconductor nanoparticles have huge attention in this field because they have good opto-electronic properties [4]. Cerium oxide has received much interest because of its unique applications. The interest in this material is because it is chemically stable and the lattice constant value is near to the silicon [5]. It has a high capability of storing as well as releasing oxygen [6] and has a cube fluorite structure [7]. Compared to other oxides, CeO_2 has become a remarkable nanoparticle due to its good index of refraction, hardness, high reactivity [8], high transmitting power within the infrared and visible range, and excellent adhesive power [9]. It is also stable during chemical damage and elevated temperatures [10].

There is a large variety of methods that have been used to form CeO_2, such as blaze sprayer, solvothermal dissolution [11], hydrothermal dissolution [12], electric-chemical assertion, co-precipitation [13], microemulsion [14] , microwave-assisted [15], polyol method [16]and sol gel method [17-19]. Among them, co-precipitation process has been considered the simple, timesaving

* Corresponding author: qamariub@gmail.com
https://doi.org/10.15251/JOR.2025.213.307

method that gives low-cost and high purity oxides in comparison to different chemical process and can be used for mass production of material [20, 21]. Scientific society is greatly interested in this material as it has a wider band gap [22]. CeO_2 nanoparticle has been successfully used for buffer layers [23], filters, solid oxide fuel cell [24], catalyst [25], antibacterial activity [26], photocatalysis [27], biomedical [28]and NO removal [29].

Different scientists have contributed to understanding the properties of CeO_2. Ramachandran, Subadevi, Sivakumar [21] synthesized CeO_2 by utilizing cerium nitrate hexahydrate ($Ce(NO_3)_3.6H_2O$) and sodium hydroxide by changing pH value from 9-12. By enhancing pH value, crystal size was reduced. Magdalane, Kaviyarasu, Raja, Arularasu, Mola, Isaev, Al-Dhabi, Arasu, Jeyaraj, Kennedy [30] synthesized Erbium doped CeO_2 NPs via hydrothermal process by using Erbium nitrate and $Ce(NO_3)_3.6H_2O$. Priyanka, Babitha, Varghese [31] formed CeO_2 NPs vis $Ce(NO_3)_3.6H_2O$ and ammonium carbonate. Mun, Park, Jeong, Lee, Oh, Seo [32] studied the electrical, optical as well as thermal properties of CeO_2 NPs that was doped with nematic liquid crystal. Farahmandjou, Zarinkamar, Firoozabadi [20] utilized potassium carbonate and $Ce(NO_3)_3.6H_2O$ to prepare CeO_2.

This work includes the formation of CeO_2 via co-precipitation process and studies the effect of calcination temperature on CeO_2 by characterizing it by XRD, SEM, FTIR, UV-Vis, PL, Raman and IV characteristics. With these characterization techniques, crystal structure, morphology, functional groups, optical features, molecular structure, and electrical properties are investigated.

2. Experimental section

To prepare CeO_2 nanoparticles, cerium nitrate hexahydrate ($Ce(NO_3)_3.6H_2O$) was used as a precursor. In this process, a 0.25 mol solution of cerium nitrate hexahydrate was formed in distilled water, and then a 1 mol solution of sodium hydroxide (NaOH) was added dropwise and stirred this solution continuously for 30 minutes. The pH is maintained during this process. There is a noticeable change in color from light brown to purple. The precipitates settled down when the solution was kept the whole night. The solution was placed in a centrifuge that had 6000 rotations per minute (rpm) for five minutes. Then, washing was done with distilled water. Precipitates were dried in the oven overnight at 60 ^{0}C. These dried precipitates changed their color from purple to pale yellow, and then they were ground by using mortar and pestle and converted into powder. The sample was calcined at different temperatures of 400 ^{0}C, 500 ^{0}C, 600 ^{0}C for 2 hours.

The crystal structure of CeO_2 was analyzed through X-ray diffraction (XRD), and was done by utilizing an X-ray diffractometer machine using Cu-Kα as a radiation source. The surface morphology was investigated through a Scanning electron microscope (SEM). Fourier Transform Infrared Spectroscopy (FTIR) identified the presence of functional groups. The optical properties and band gap of the formed CeO_2 were examined through Ultraviolet and Visible spectroscopy (UV-Vis) and photoluminescence (PL). The molecular structure was analyzed via Raman spectroscopy. The electrical properties of CeO_2 were characterized by IV characteristics.

3. Result and discussion

3.1. Structural analysis

XRD patterns identified the crystalline structure of the CeO_2. *Fig. 1* indicates the XRD results of as-synthesize CeO_2 samples and calcined at 400, 500, and 600 ^{0}C temperatures. These patterns confirmed the cube fluorite structure having (111) oriented plane. The Millar indices of (111), (200), (220), and (311) were also obtained, which indicated the cube nature of CeO_2. All these peaks of CeO_2 showed good agreement with formerly reported literature [20, 33]. There was no remarkable peak that confirmed the Ce_2O_3 crystal structure. Therefore, it exhibited the phase nature of nanoceria [4]. The effect of calcination temperature on particle size and lattice constant is shown in *Fig. 2.* The variations in calcination temperature powerfully affected the particle size and lattice constant. It is observed that as calcination temperature was increased, particle size and lattice

constant also increased linearly *(Table 1).* As oxygen vacancies increased in it the value of lattice parameters in nanoparticles was also high [18]. Bragg's law calculated the d-value of the samples:

$$2d_{hkl}\sin\theta_{hkl}=n\lambda$$

CeO_2 particle size was calculated via the Scherrer equation [34].

$$D=\frac{0.9\lambda}{\beta\cos\theta}$$

where β indicates full width at half maxima (FWHM) value in radians, θ indicates angle measure in radians and λ indicates wavelength of x-rays. The standard value of λ is 1.54059.

The lattice constant 'a' was determined through

$$a=d(h^2+k^2+l^2)^{1/2}=\frac{\lambda}{2\sin\theta}(h^2+k^2+l^2)^{1/2}$$

Here, (hkl) shows millar indices and d shows spacing between planes of a cube.

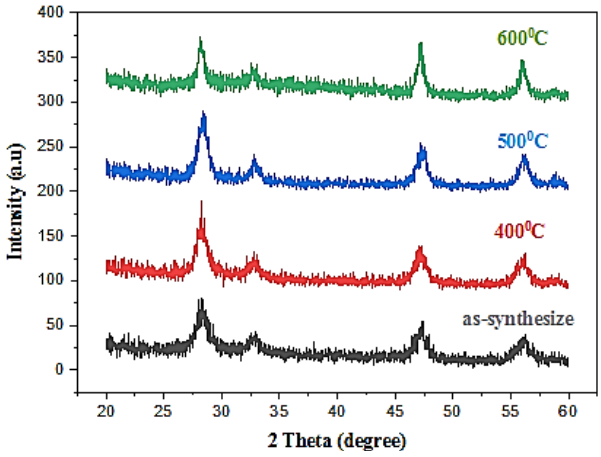

Fig. 1. XRD Pattern of CeO_2 NPs (as-synthesize at 400⁰C, 500⁰C, 600⁰C).

The particle size varies from 60-90nm when calcination temperature increases, i.e., particle size also increases.

Table 1. Analysis of XRD for as-synthesized samples, calcined at 400, 500 and 600 ^{0}C.

Sample name	Angle (2θ degree)	d-Value A^0	Intensity (a.u)	FWHM (2θ degree)	Millar indices (hkl)	Lattice Constants 'a' A^0	Particle size (nm)	X-ray Density g/cm^3
As-synthesized	28.281	3.153	66.9	1.781	111	5.461	46.004	7.021
	32.403	2.761	32.86	3.224	200	5.522	25.661	6.794
	47.214	1.924	42.27	1.089	220	5.441	79.606	7.102
	56.0811	1.639	31.07	0.884	311	5.435	101.848	7.125
Calcined at 400 ^{0}C	28.271	3.154	70.81	1.551	111	5.463	52.82	7.014
	32.511	2.752	32.81	2.486	200	5.504	33.293	6.86
	47.169	1.925	39.81	1.077	220	5.445	80.497	7.082
	56.006	1.641	33.90	0.92	311	5.441	97.752	7.099
Calcined at 500 ^{0}C	28.36	3.144	81.72	1.214	111	5.446	67.513	7.079
	32.826	2.726	34.36	1.043	200	5.452	79.418	7.056
	47.286	1.921	44.45	0.959	220	5.433	90.473	7.132
	56.125	1.637	37.27	0.858	311	5.431	104.88	7.14
Calcined at 600 ^{0}C	28.21	3.161	64.45	0.673	111	5.475	121.63	6.969
	32.68	3.161	37.54	36.46	200	5.474	2.2704	6.965
	47.194	1.924	58.55	0.787	220	5.443	112.86	7.093
	51.142	1.785	43.81	0.79	311	5.437	112.78	7.114

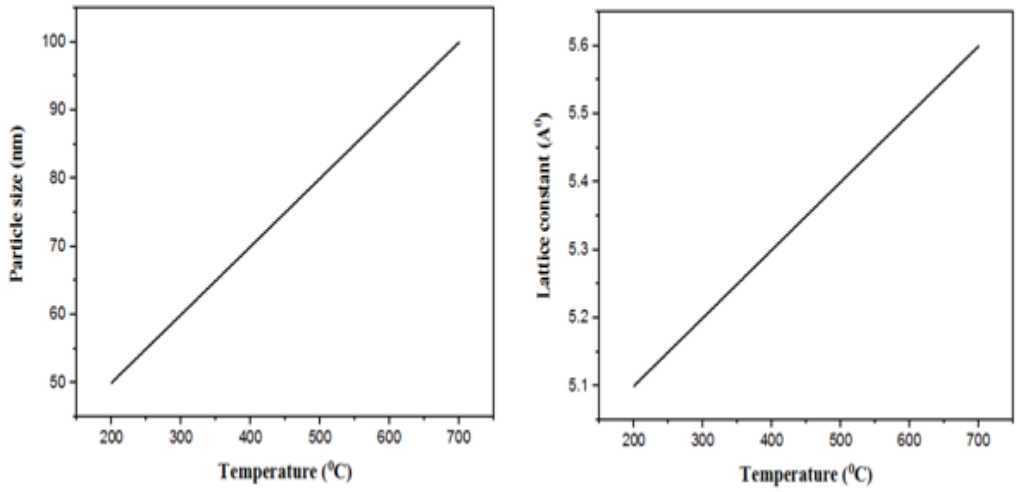

Fig. 2. Variation of calcinations temperature with particle size and lattice constant.

3.2. Morphological analysis

Fig. 3(a) shows the SEM image of as-synthesized CeO_2 that were prepared via co-precipitation method. SEM micrographs of CeO_2 that were calcined at 400, 500 and 600 ^{0}C, shown in Fig. 3 (b-d) respectively. SEM micrograph of as-prepared CeO_2 indicates the agglomeration of the particles. The particles are in the form of clusters and are in spherical shape. Surface morphology shows that as calcination temperature is increased, the surface became non-homogeneous. Particles

show non-uniform clumped distribution having rough surfaces. The particle size vary from 70-100nm as calcinations temperature is increased.

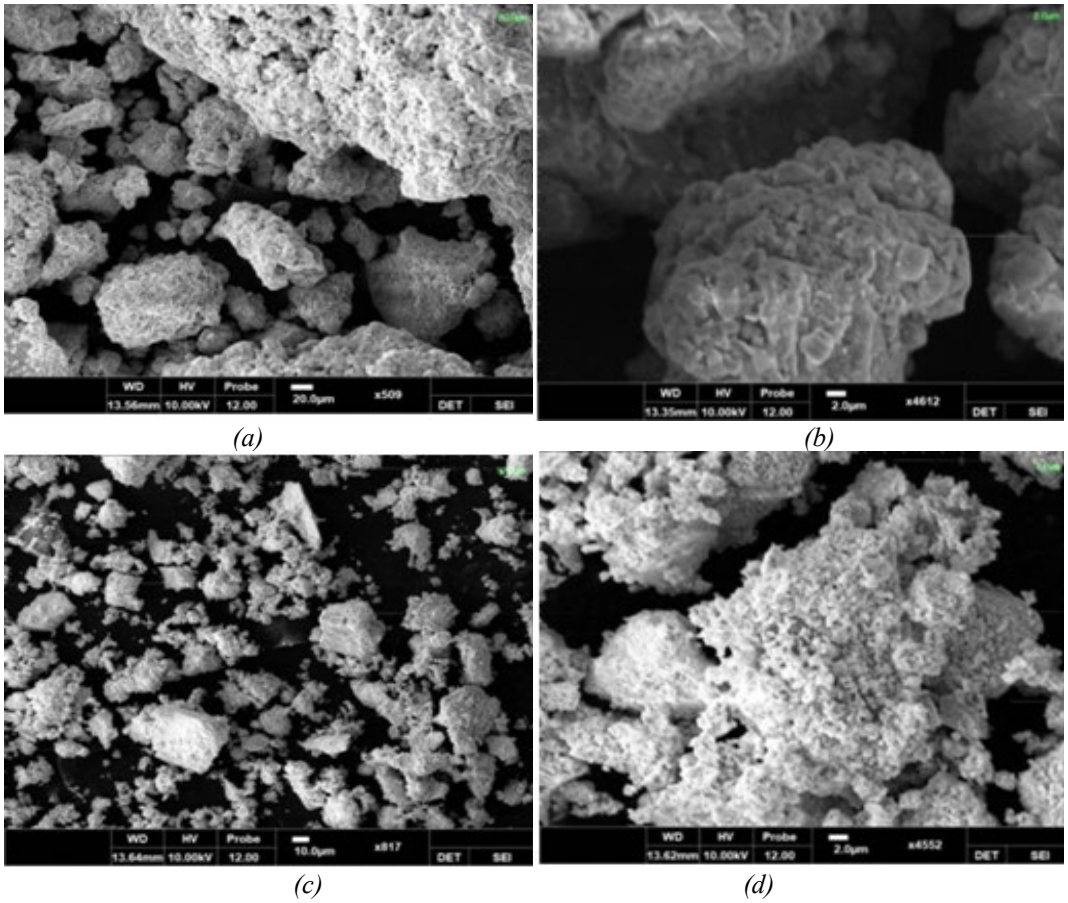

Fig. 3. Scanning Electron Micrographs for CeO_2 (a) As-synthesized (b) calcined at 400 ^{0}C (c) calcined at 500 ^{0}C (d) calcined at 600 ^{0}C

3.3. Functional group analysis

The functional groups of CeO_2 NPs were observed via FTIR spectra. *Fig. 4* shows the FTIR spectra of as-synthesized CeO_2, calcined at 400, 500 and 600 ^{0}C. These spectra show the major absorption bands of CeO_2. In nanoceria samples, the band near 400-550 cm^{-1} is because of the metal oxide (Ce-O) bond [35, 36]. These lattice oscillations indicate cube CeO_2 bonds. The bands present below 700 cm^{-1} are due to Ce-O bonds [37].

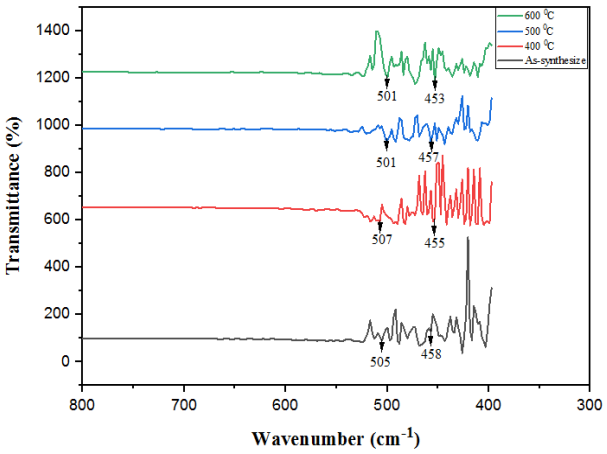

Fig. 4. FTIR analysis for as-synthesized CeO_2, calcined at 400, 500, 600 ^0C.

3.4. Optical analysis

The absorption band and band gap of CeO_2 were determined via the Ultraviolet and visible absorption spectrum. The UV-Vis spectra of CeO_2 NPs and band gap spectra are displayed in *Fig. 5.* The electronic optical band gap is observed with UV-Vis spectroscopy. *Fig. 5 (a, b, c, d)* shows the UV-Vis spectra of as-prepared CeO_2 and calcined CeO_2 at 400, 500 and 600 ^0C respectively. All samples have an absorption band at 236 nm. The band gap in UV-Vis spectroscopy was found via the Tauc method and by using the formula [38].

$$E_{BG} = \frac{1240}{\lambda_{AbsorbEdge}}$$

where E_{BG} indicates energy of band gap and $\lambda_{AbsorbEdge}$ indicates absorption edge wavelength. The value of band gap was found to be 3.27 eV.

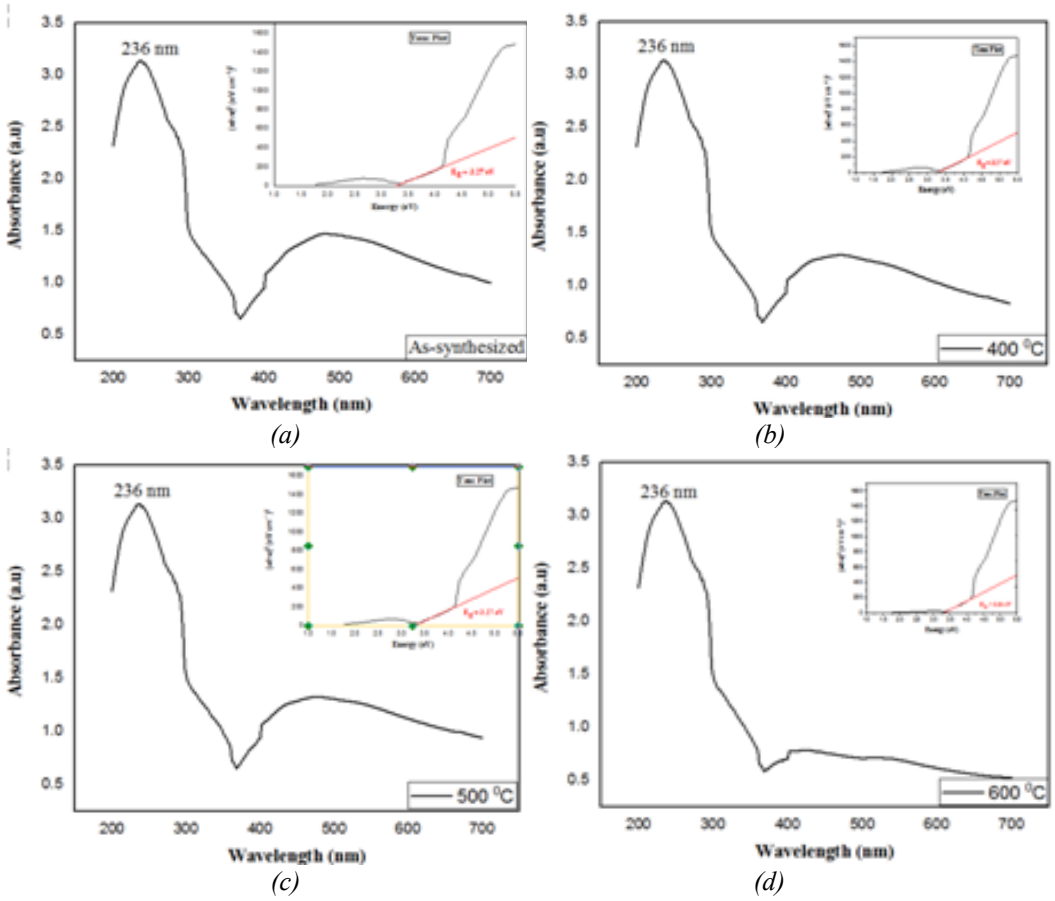

Fig. 5. UV-Vis analysis for (a) As-synthesized CeO_2 (b) calcined at 400 ^{0}C (c) calcined at 500 ^{0}C (d) calcined at 600 ^{0}C

3.5. PL analysis

Photoluminescence spectra of as-synthesized and calcined CeO_2 were observed at 630 nm excitation wavelength and are shown in *Fig. 6.* The emission of PL around 640-660 nm is related to the transfer of charge from the energy state of Ce 4f to the energy state of O 2p. This localized energy state within 4f of Ce and 2p of O because of imperfections is responsible for wide emission band [39]. All the samples of CeO_2 have an emission band at 651 nm wavelength. As the calcination temperature increased, the peak position did not change; however, the peak became sharper. The band gap of PL spectra is found to be 1.90 eV. This PL spectra helps to observe imperfective oxygen found within CeO_2, charge transfer from 4f sub shell to 2p valance shell of CeO_2, surface impurity, as well as energy state defects present between Ce 4f and O 2p.

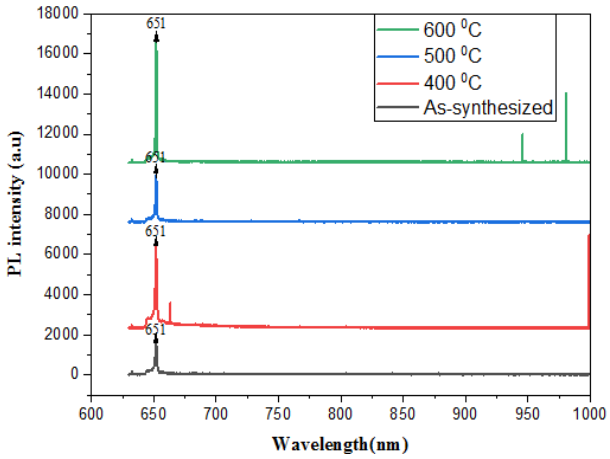

Fig. 6. PL analysis for as-synthesized CeO_2, calcined at 400, 500, 600 ^0C.

3.6. Raman spectroscopy

Fig. 7 indicates the Raman spectra of as- synthesized CeO_2 and calcined CeO_2 at 400, 500 and 600 ^0C. CeO_2 showed cube fluorite nature, so it has one vibration mode at Raman shift value of 464 cm^{-1} [40]. The cubic CeO_2 was confirmed by this single peak. This has an F_{2g} distribution and could be seen as the 'symmetric breathing mode' of the oxygen atom. These oxygen atoms surround every positive ion. The vibrating mode does not depend upon the mass of positive ions because only oxygen atoms are mobile [41]. As-prepared CeO_2 has a Raman peak at 457 cm^{-1}. The peak is shifted a little bit forward and sharper as calcinations temperature is enhanced. At 400 ^0C, Raman peak is at 459 cm^{-1}, for 500 ^0C Raman peak shifts at 462 $cm^{-1,}$ and for 600 ^0C Raman peak is at 462 cm^{-1}.

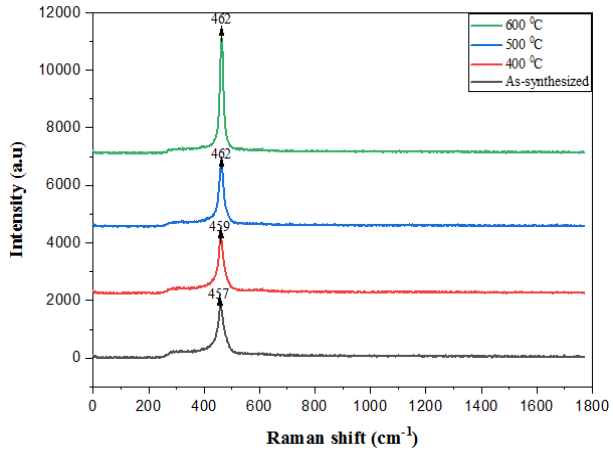

Fig. 7. Raman analysis for as-synthesized CeO_2, calcined at 400, 500, 600 ^0C.

3.7. Electrical analysis

The electrical resistivity for the CeO_2 was obtained by using the formula

$$\rho=\frac{RA}{L}$$

here, R is the resistance, A is area and L is thickness of the pellets. To examine the electric properties of the formed samples, I-V studies were employed with the help of two probe methods. The change in current at constant voltage was observed at various temperatures of 40-200 ^{0}C for the entire range of samples. Fig. 8(a-d) shows the I-V graph for as-synthesized nanoceria and calcined at 400, 500 and 600 ^{0}C respectively.

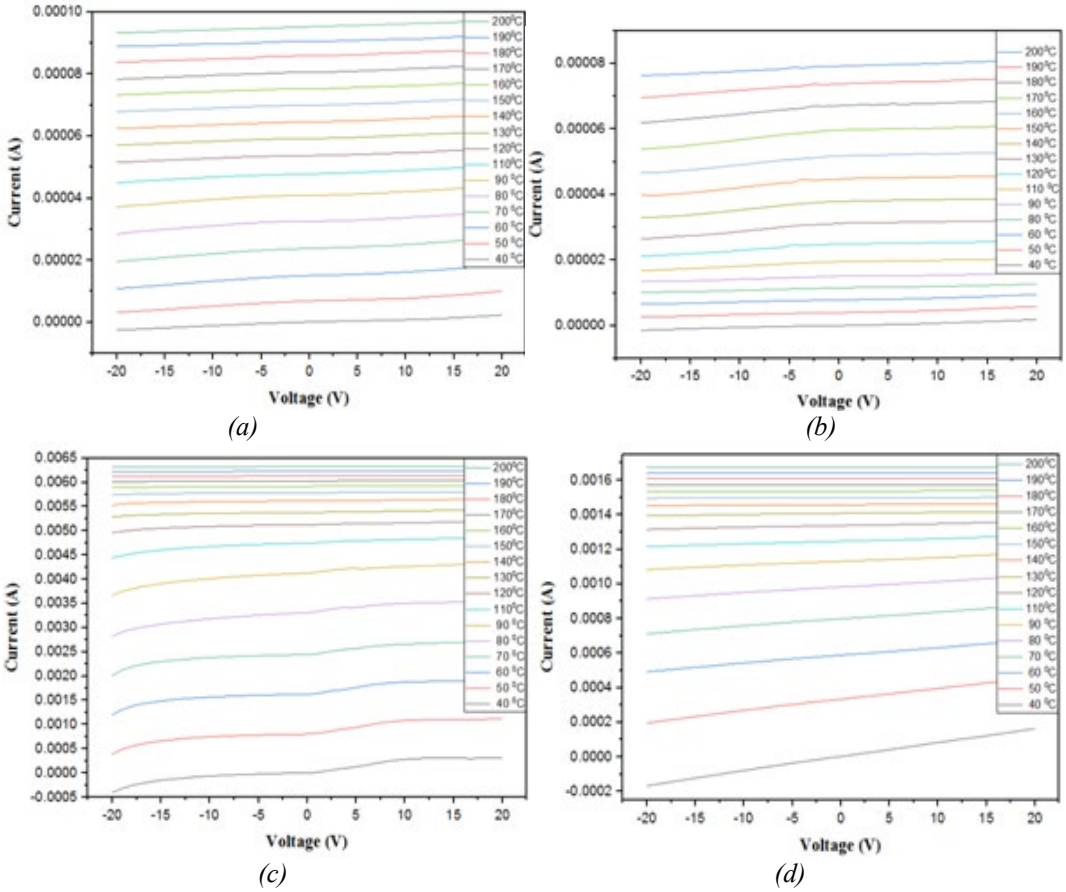

Fig. 8. I-V curve for as-synthesized CeO_2, calcined at 400, 500, 600 ^{0}C.

Fig. 9 (a) shows the relation of temperature and resistivity for the nanoceria samples. The value of resistivity is small for the as-prepared sample, but when the calcination temperature was increased, the value of resistivity also increased. In starting, resistivity increases, but at a specific level of kelvin temperature, resistivity falls. Its value was calculated by using the above equation and is in the range of 7.8×10^6- 2.1×10^8 ohm-cm. Fig. 9 (b) shows the relation of temperature with log of resistivity to smooth the values and to eliminate the power of resistivity. This graph also shows that resistivity increases by increasing the calcination temperature.

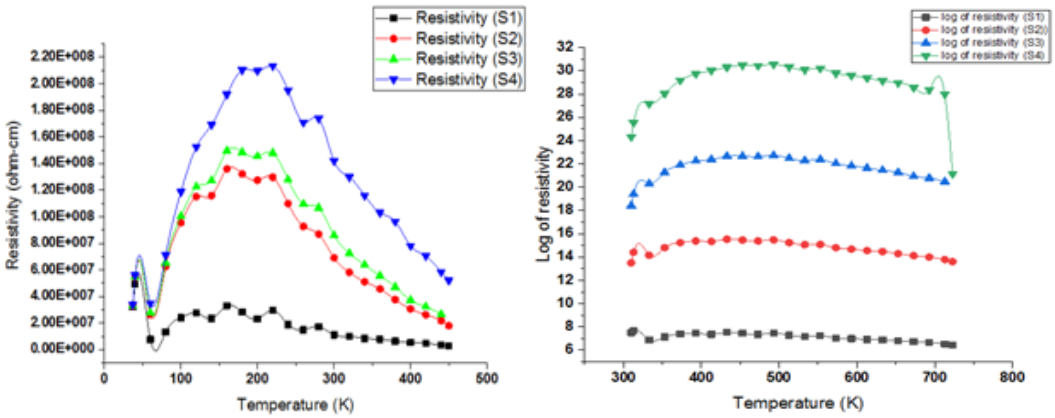

Fig. 9. Relation of temperature with resistivity and log of resistivity for as-synthesized CeO_2, calcined at 400, 500, 600 ^0C.

4. Conclusion

The formation and influence of calcination temperature over CeO_2 nanoparticles were analysed. CeO_2 was formed by the co-precipitation method using cerium nitrate hexahydrate as the starting material. The nanoparticles were investigated through XRD, SEM, FTIR, UV-Vis, PL, Raman and IV. XRD indicated that particle size increases by increasing the calcination temperature. SEM revealed non-uniform clumped distribution having rough surfaces. FTIR showed the metal oxide (Ce-O) bond in nanoceria. UV-Vis showed the absorption wavelength occurs at 236 nm with energy band gap of 3.27 eV. PL indicated that the emission band is present at 651 nm wavelength with 1.90 eV band gap. Raman peak showed the cube fluorite structure of CeO_2. I-V studies indicated that the resistivity was in the range of 7.8×10^6- 2.1×10^8 ohm-cm and increases with calcinations temperature.

References

[1] S. Golovynskyi. Ukrine Journal of Physics Optics 25(1), 01045 (2024); https://doi.org/10.3116/16091833/24/5/S1/2023

[2] I. R. De Larramendi, Ortiz-Vitoriano N., Acebedo B., De Aberasturi D. J., De Muro I. G., Arango A., Rodríguez-Castellón E., De Larramendi J. I. R., Rojo T., International Journal of Hydrogen Energy 36(17), 10981 (2011); https://doi.org/10.1016/j.ijhydene.2011.05.177

[3] F. Findik, Periodicals of Engineering and Natural Sciences 9(3),62 (2021); https://doi.org/10.21533/pen.v9i3.1837

[4] N. K. Renuka, Journal of Alloys and Compounds 513, 230 (2012); https://doi.org/10.1016/j.jallcom.2011.10.027

[5] S. Wang, Wang W., Zuo J., Qian Y., Materials Chemistry and Physics 68(1-3), 246 (2001); https://doi.org/10.1016/S0254-0584(00)00357-6

[6] F. Bao, Han X., Liu K., Zhang Z., Sun L., Rao C., Zhang Y., Yang X., Solid State Ionics 415, 116654 (2024); https://doi.org/10.1016/j.ssi.2024.116654

[7] J. R. Vargas-Garcia, Beltran-Romero L., Tu R., Goto T., Thin Solid Films 519(1), 1 (2010); https://doi.org/10.1016/j.tsf.2010.06.057

[8] V. Pathak, Lad P., Thakkar A. B., Thakor P., Deshpande M., Pandya S., Results in Surfaces and Interfaces 11, 100111 (2023); https://doi.org/10.1016/j.rsurfi.2023.100111

[9] S. Singh, Jain R. K. Cureus 16(1) (2024); https://doi.org/10.7759/cureus.52177

[10] F. Zhang, Chan S.-W., Spanier J. E., Apak E., Jin Q., Robinson R. D., Herman I. P., Applied physics letters 80(1), 127 (2002); https://doi.org/10.1063/1.1430502

[11] Y. Sun, Lu X., Huang Y., Wang G., Nanomaterials 14(10), 812 (2024); https://doi.org/10.3390/nano14100812

[12] Y. Xu, Zhou Y., Li Y., Liu Y., Ding Z., Journal of Environmental Chemical Engineering:113719 (2024); https://doi.org/10.1016/j.jece.2024.113719

[13] S. Aseena, Abraham N., Babu V. S., Materials Today: Proceedings 80, 1901 (2023); https://doi.org/10.1016/j.matpr.2021.05.636

[14] N. Mehrooz, Gharibshahi R., Jafari A., Shadan B., Delavari H., Sadeghnejad S., Scientific Reports 14(1), 11652 (2024); https://doi.org/10.1038/s41598-024-62393-5

[15] S. Vijaya, Kennedy L. J., Fuel 373, 132354 (2024); https://doi.org/10.1016/j.fuel.2024.132354

[16] G. Anello, Di Felice L., Gallucci F.; https://doi.org/10.1016/j.catcom.2022.106491

[17] C. Y. Jimmy, Zhang L., Lin J., Journal of colloid and interface science 260(1), 240 (2003); https://doi.org/10.1016/S0021-9797(02)00168-6

[18] N. S. Arul, Mangalaraj D., Chen P. C., Ponpandian N., Viswanathan C. Materials Letters 65(17-18), 2635 (2011); https://doi.org/10.1016/j.matlet.2011.05.022

[19] C. Gao, Sun H., Du J., Angewandte Chemie International Edition 64(7), e202420079 (2025); doi: https://doi.org/10.1002/anie.202420079

[20] M. Farahmandjou, Zarinkamar M., Firoozabadi T., Revista mexicana de física 62(5), 496 (2016); ttps://www.scielo.org.mx/scielo.php?script=sci_abstract&pid=S0035-001X2016000500496&lng=en&nrm=iso

[21] M. Ramachandran, Subadevi R., Sivakumar M. Vacuum 161, 220 (2019); https://doi.org/10.1016/j.vacuum.2018.12.002

[22] M. Isik, Delice S., Gasanly N., Physica E: Low-dimensional Systems and Nanostructures 150, 115712 (2023); https://doi.org/10.1016/j.physe.2023.115712

[23] Z. Dong, Zhou C., Chen W., Lin F., Luo H., Sun Z., Huang Q., Zeng R., Tan Y., Xiao Z., Advanced Functional Materials 34 (34), 2400809 (2024); https://doi.org/10.1002/adfm.202400809

[24] Y. Lan, Wang L., Luo Y., Hao R., Zhang H., Aruta C., Yang F., Yu Y., Yang N. Journal of the European Ceramic Society 44(2), 996 (2024); https://doi.org/10.1016/j.jeurceramsoc.2023.10.002

[25] S. Li, Li J., Liang W., Cai J., Guo R., Journal of Environmental Chemical Engineering 12(5), 113528 (2024); https://doi.org/10.1016/j.jece.2024.113528

[26] A. B. Shcherbakov, European Journal of Medicinal Chemistry Reports 10, 100141 (2024); https://doi.org/10.1016/j.ejmcr.2024.100141

[27] K. A. Hoque, Sathi S. A., Akter F., Akter T., Ahmed T., Ullah W., Arafin K., Rahaman M. S., Shahadat H. M., Imran A. B., Journal of Environmental Chemical Engineering 12(5),113487 (2024); https://doi.org/10.1016/j.inoche.2023.111738

[28] V. Pathak, Lad P., Thakkar A. B., Thakor P., Deshpande M., Pandya S., Inorganic Chemistry Communications 159, 111738 (2024); https://doi.org/10.1016/j.inoche.2023.111738

[29] A. Kumar, Babu S., Karakoti A. S., Schulte A., Seal S., Langmuir 25(18), 10998 (2009); https://doi.org/10.1021/la901298q

[30] C. M. Magdalane, Kaviyarasu K., Raja A., Arularasu M., Mola G. T., Isaev A. B., Al-Dhabi N. A., Arasu M. V., Jeyaraj B., Kennedy J., Journal of Photochemistry and Photobiology B: Biology 185, 275 (2018); https://doi.org/10.1016/j.jphotobiol.2018.06.011

[31] B. K. Priyanka, T. Varghese, Synthesis, characterization and electrical properties of cerium oxide nanoparticles, Taylor & Francis, 61, 2018.

[32] H.-Y. Mun, Park H.-G., Jeong H.-C., Lee J. H., Oh B.-Y., Seo D.-S., Liquid Crystals 44(3), 538 (2017);https://doi.org/10.1080/02678292.2016.1225838

[33] J.-C. Chen, Chen W.-C., Tien Y.-C., Shih C.-J., Journal of alloys and compounds 496(1-2), 364 (2010); https://doi.org/10.1016/j.jallcom.2010.01.151

[34] P. Vasudevan. Journal of Molecular Structure 1272, 134144 (2023); https://doi.org/10.1016/j.molstruc.2022.134144

[35] Zhang, Kleinstreuer C., Donohue J. F., Kim C., Journal of aerosol science 36(2), 211 (2005); https://doi.org/10.1016/j.jaerosci.2004.08.006

[36] M. Zawadzki, Journal of Alloys and Compounds 454(1-2), 347 (2008); https://doi.org/10.1016/j.jallcom.2006.12.078

[37] R. Deus, Cilense M., Foschini C., Ramirez M., Longo E., Simões A. Journal of alloys and compounds 550, 245 (2013); https://doi.org/10.1016/j.jallcom.2012.10.001

[38] Chen, Li F., Yu J. Materials Letters 60(1), 57 (2006); https://doi.org/10.1016/j.matlet.2005.07.088

[39] C. Sun, Li H., Zhang H., Wang Z., Chen L. Nanotechnology 16(9), 1454 (2005); https://doi.org/10.1088/0957-4484/16/9/006

[40] M. Dos Santos, Lima R., Riccardi C., Tranquilin R., Bueno P. R., Varela J. A., Longo E. Materials Letters 62(30), 4509 (2008); https://doi.org/10.1016/j.matlet.2008.08.011

[41] D. M. D. M. Prabaharan, Sadaiyandi K., Mahendran M., Sagadevan S. Materials Research, 19(2), 478 (2016); https://doi.org/10.1590/1980-5373-MR-2015-0698